

A Modified Bounding Surface Hypoplasticity Model for Sands

Gang Wang* and Yongning Xie

Department of Civil and Environmental Engineering
Hong Kong University of Science and Technology
Clearwater Bay, Kowloon, Hong Kong SAR, China
gwang@ust.hk

Abstract. A modified bounding surface hypoplasticity model is developed to capture distinct dilatancy behaviors of sandy soils during various phases of cyclic loading. The model features a new modulus formulation, a phase transformation surface that is dependent on a state variable and soil density. The effects of accumulated plastic strains on the plastic moduli are also considered. The modified model improves simulation of cyclic mobility and post-liquefaction behavior of both loose and dense sands. The model capacity is demonstrated by comparing the model simulations with a series of undrained cyclic simple shear tests on Fraser River sand.

Keywords: constitutive model, bounding surface hypoplasticity, cyclic response.

1 Introduction

Much progress has been made during the past thirty years to develop advanced constitutive models to simulate the fundamental stress-strain-strength relationships of granular soils. Among them, the bounding surface model developed by Wang *et al.* [1] has been successfully used to simulate fully nonlinear site response [2] and earthquake-induced liquefaction and deformation of earth structures [3]. However, the original model suffers several drawbacks. The model does not prescribe a zero dilatancy at the limit of critical state. Therefore, it is not consistent with the critical state theory and can not properly characterize the dilatancy behavior in liquefied state. Although the original model can simulate cyclic response of loose sands reasonably well, it can not properly model the dilatancy behavior and the cyclic mobility of dense sands. To overcome these difficulties, a modified bounding surface hypoplasticity model based on the original framework of Wang *et al.* [1] is developed in this study.

2 Model Formulation

Following [1], the effective stress is represented by the deviatoric stress ratio $\mathbf{r} = \mathbf{s}/p$, where $\mathbf{s} = \boldsymbol{\sigma} - p\mathbf{I}$ is the deviatoric stress tensor, $p = 1/3tr(\boldsymbol{\sigma})$ is the mean

* Corresponding author.

effective stress. The stress ratio invariant, $R = \sqrt{1/2\mathbf{r} : \mathbf{r}}$, is used to define the following bounding surfaces: The failure surface R_f , which defines the ultimate limit of an admissible R ; The maximum prestress surface R_m , which defines the maximum stress ratio experienced by the material. The phase transformation surface R_p , which defines the location where transformation from contractive to dilative behavior occurs. These bounding surfaces are illustrated in the $p - J$ space (where $J = \sqrt{1/2\mathbf{s} : \mathbf{s}} = pR$) and stress ratio space in Fig. 1. In Fig. 1(b), the current stress state is represented by vector \mathbf{r} . A projection center α is defined as the last stress reversal point, or is set to the origin if the current stress state exceeds the maximum pre-stress surface R_m , i.e., virgin loading. An image stress point $\bar{\mathbf{r}}$ is defined as the point projected on the R_m surface from the projection center α through the current stress state point \mathbf{r} . Scaler quantities ρ and $\bar{\rho}$ measure the distances between α , \mathbf{r} and $\bar{\mathbf{r}}$, and their ratio $\bar{\rho}/\rho$ will be used in the plastic shear modulus formulation.

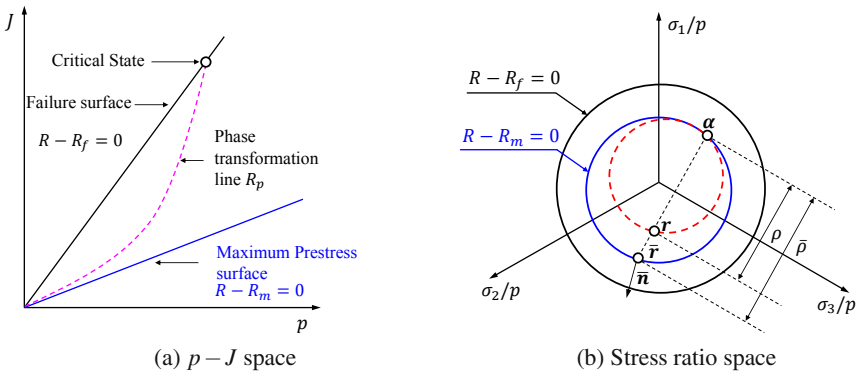


Fig. 1. Bounding surfaces in $p - J$ space and stress ratio space

The concept of state-dependent dilatancy assumes that R_p follows the following relationship [4]:

$$R_p = R_f e^{m\psi} \quad (1)$$

where ψ is a state parameter defined as the difference between the current void ratio e_0 and the critical void ratio e_c in Fig. 2. e_c is related to the current mean effective stress p through the following equation [5]:

$$e_c = e_\Gamma - \lambda \left(\frac{p}{p_a} \right)^\xi \quad (2)$$

where e_Γ , λ and ξ are critical state parameters. By examining the laboratory test data, a single value can not be assigned to m to realistically represent the phase transformation lines of both loose and dense samples. In this study, m is proposed

to be dependent on the relative density of the sample. Fig. 3 illustrates the phase transformation lines for dense ($m = 4$, $D_r = 80\%$) and relatively loose ($m = 1.2$, $D_r = 40\%$) samples of Fraser River sands. By comparison, the transformation line of the loose sample is much closer to the failure line, indicating it is more contractive than the dense sample.

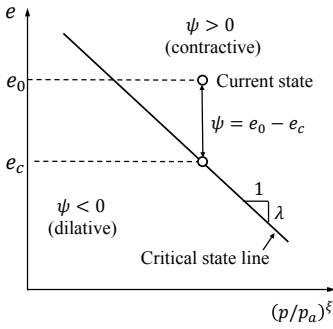


Fig. 2. Critical state line

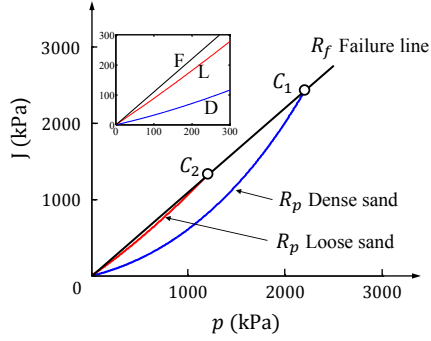


Fig. 3. Phase transformation line

The elastic stress-strain relationship can be written as:

$$\dot{\boldsymbol{\epsilon}}^e = \dot{\boldsymbol{\epsilon}}^e + \frac{1}{3}(tr\dot{\boldsymbol{\epsilon}}^e)\mathbf{I} = \frac{1}{2G}\dot{\mathbf{s}} + \frac{1}{3}\dot{p}\mathbf{I} = \frac{1}{2G}p\dot{\mathbf{r}} + \left(\frac{1}{2G}\mathbf{r} + \frac{1}{3K}\mathbf{I}\right)\dot{p} \quad (3)$$

where G and K are elastic shear and bulk moduli, respectively. In this paper, only the plastic strain rate induced by $p\dot{\mathbf{r}}$ will be considered for simplicity:

$$\dot{\boldsymbol{\epsilon}}^p = \left(\frac{1}{H_r}\bar{\mathbf{n}} + \frac{1}{3K_r}\mathbf{I}\right)(p\dot{\mathbf{r}} : \bar{\mathbf{n}}) \quad (4)$$

where H_r and K_r are plastic shear and bulk moduli associated with the deviatoric and volumetric plastic strains. The $\bar{\mathbf{n}}$ is a deviatoric unit tensor specifying the direction of deviatoric plastic strain rate, defined here as normal to the maximum prestress surface at the image point $\bar{\mathbf{r}}$ in Fig. 1(b). The $p\dot{\mathbf{r}} : \bar{\mathbf{n}}$ is loading index. The plastic shear modulus H_r is defined as:

$$H_r = Gh_r C_H(\xi_q) \left[\frac{R_f}{R_m} \left(\frac{\bar{\rho}}{\rho}\right) - 1 \right] \left(\frac{p}{p_m}\right)^{1/2} \quad (5)$$

where

$$C_H(\xi_q) = \frac{1}{1 + \alpha\xi_q} \quad \text{and} \quad \xi_q = \int_0^{e^p} \sqrt{\frac{2}{3}d\mathbf{e}^p : d\mathbf{e}^p} \quad (6)$$

h_r is a dimensionless material constant, $C_H(\xi_q)$ accounts for the influence of accumulated deviatoric plastic strain, ξ_q , on the plastic modulus ($d\mathbf{e}^p$ is the deviatoric

plastic strain increment). Parameter α is used to control the extent of the strain dependence. The strain-dependent term is essential to effectively represent the cyclic mobility. Without the strain-dependent term, a stabilized cyclic stress-strain behavior will eventually be reached under a repeated cyclic loading. Parameter α is used to control the extent of the strain dependence. A pressure-dependent term $(p/p_m)^{1/2}$ is included to strengthen the influence of the mean effective stress on the plastic shear modulus, and it can effectively improve the stress-strain hysteresis behaviors.

The plastic bulk modulus K_r is formulated by modifying the elastic bulk modulus K as follows:

$$K_r = p_a \frac{1 + e_{in}}{wK} \left(\frac{p}{p_a} \right)^{1/2} = \frac{K}{w} \quad (7)$$

where

$$w = \begin{cases} w_1 = \frac{1}{k_r} \left(\frac{R_m}{R_f} \right)^b \left(\frac{R_p - R}{R_f - R_m} \right), & \text{if } R = R_m \text{ or } R > R_p, \text{ and } \dot{R} > 0 \quad (8a) \\ w_2 = C_K(\xi_v) \left(\frac{R_m + \text{sign}(\dot{R})R}{R_f} \right) \left(\frac{R_p - \text{sign}(\dot{R})R}{R_p + R_m} \right), & \text{otherwise.} \quad (8b) \end{cases}$$

The above formulation controls the volumetric dilatancy of sands. It is noted that w_2 always assume a non-negative value and is used only for a contactive phase. w_1 is used for all dilative phases, but it can also be used prescribe a contractive response if $R = R_m$ (virgin loading) and $R < R_p$. The parameter $C_K(\xi_v) = d_1(1 + d_2 \tanh(100 \xi_v))$, where ξ_v is the plastic volumetric strains accumulated only during dialtive phases, d_1 and d_2 are model parameters whose values may vary with different relative densities. The function \tanh is used to prescribe a maximum value of the strain-dependent effect.

3 Model Simulations

The performance of the proposed model is demonstrated through comparison with a series of cyclic simple shear tests on Fraser River sand conducted at UBC [6]. The test samples were densified to a relative density (D_r) of 40% and 81% under applied pressues of 100 kPa and 200 kPa, respectively. Samples were then subjected to cyclic shear for a range of cyclic stress ratios (CSR) under constant volume conditions that simulate the undrained response. The calibrated model parameters are summarized in Table 1. The test data and model simulations are presented in Figs. 4 to 5. During the first a few loading cycles, the dense sample ($D_r = 81\%$) exhibits an increasingly stronger contractive phase following each dilative phase. As the effective stress approaches zero, the stress path is repeated following a ‘butterfly’ loop. The shear strain progressively accumulates during each loading cycles, referred to as cyclic mobility. The shape of the stress-strain curve also progressively changes to form a ‘banana’ pattern. On the other hand, the loose sample ($D_r = 40\%$) exhibits

a purely contractive response and continuous reduction of effective stress during the first six cycles. Once the effective stress approaches zero, large cyclic strains suddenly developed. The proposed model demonstrated excellent capability in simulating the effective stress paths and stress-strain behaviors of both dense and loose soil samples.

Table 1. Summary of model parameters

Critical state parameters	Phase transformation parameters	Elastic moduli parameters	Plastic shear modulus parameters	Plastic bulk modulus parameters
$e_{\Gamma} = 1.029$	$m = 4$	$G_0 = 208$	$h_r = 0.1$	$k_r = 0.3, \quad b = 0.6$
$\lambda = 0.0404$	$(D_r = 81\%)$	$\nu = 0.05$	$\alpha = 1.5$	$d_1 = 4 \quad (D_r = 81\%)$
$\xi = 0.7$	$m = 1.2$			$d_1 = 1.2$
$R_f = 0.768$	$(D_r = 40\%)$			$(D_r = 40\%)$
				$d_2 = 2$

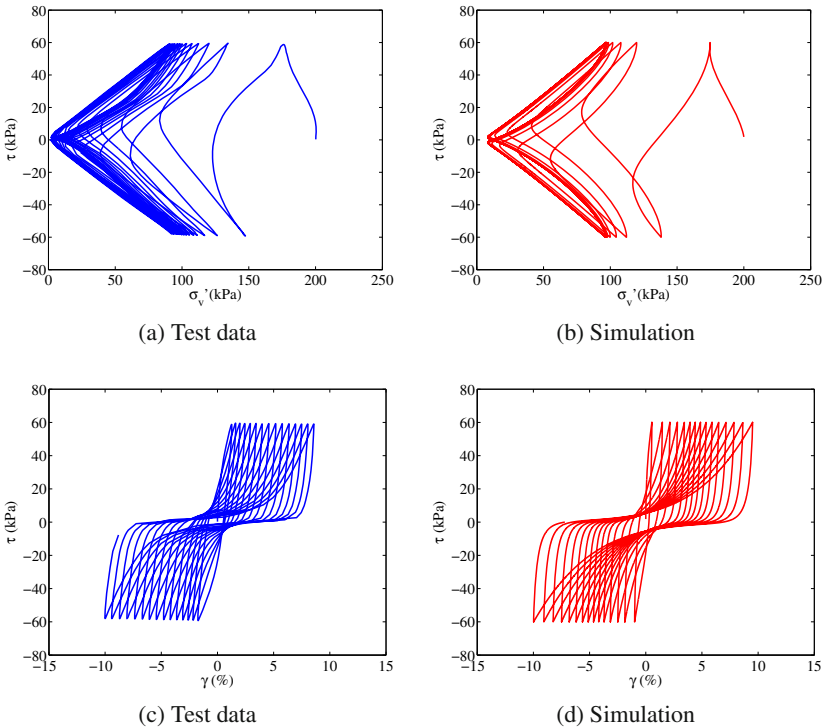


Fig. 4. Comparison of test data and model simulation for $D_r = 81\%$, $p'_0 = 200kPa$, $CSR = 0.3$. (a)(b) effective stress path, (c)(d) stress-strain curve

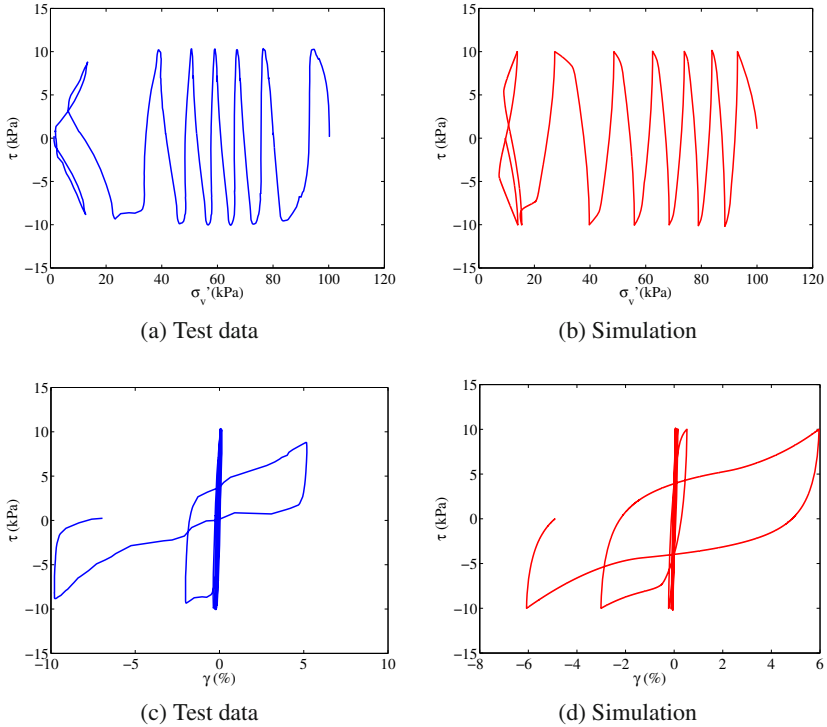


Fig. 5. Comparison of test data model simulation for $D_r = 40\%$, $p'_0 = 100\text{kPa}$, $CSR = 0.1$. (a)(b) effective stress path, (c)(d) stress-strain curve

4 Conclusions

The modified bounding surface hypoplasticity model employs a new modulus formulation that improves the simulation of distinct dilatancy behaviors of sandy soils during various phases of cyclic loading. The model demonstrated excellent performance in simulating cyclic mobility and post-liquefaction behavior of both loose and dense sands.

References

1. Wang, Z.L., Dafalias, Y.F., Shen, C.K.: Bounding surface hypoplasticity model for sand. *Journal of Engineering Mechanics* 116(5), 983–1001 (1990)
2. Li, X.S., Wang, Z.L., Shen, C.K.: A nonlinear procedure for response analysis of horizontally-layered sites subjected to multi-directional earthquake loading. Department of Civil Engineering, University of California, Davis (1992)
3. Wang, Z.L., Makdisi, F.I., Egan, J.: Practical applications of a nonlinear approach to analysis of earthquake-induced liquefaction and deformation of earth structures. *Soil Dynamics and Earthquake Engineering* 26, 231–252 (2006)

4. Li, X.S., Dafalias, Y.F., Wang, Z.L.: State-dependent dilatancy in critical-state constitutive modelling of sand. *Canadian Geotechnical Journal* 36, 599–611 (1999)
5. Li, X.S., Wang, Y.: Linear representation of steady-state line for sand. *Journal of Geotechnical and Geoenvironmental Engineering* 124(12), 1215–1217 (1998)
6. Sriskandakumar, S.: Cyclic loading response of Fraser River sand for validation of numerical models simulating centrifuge tests, Master's thesis. The University of British Columbia (2004)